

Supporting information

Impact of solid state form on the disproportionation of miconazole mesylate salt

Mitulkumar A. Patel¹, Suman Luthra², Sheri L. Shamblin³, Kapildev Arora³, Joseph F.

Krzyzaniak³, and Lynne S. Taylor^{1}*

¹Department of Industrial and Physical Pharmacy, College of Pharmacy, Purdue University,
West Lafayette, Indiana, 47907, United States.

²Pfizer Inc, Worldwide Research and Development, Cambridge, Massachusetts, United States.

³Pfizer Inc, Worldwide Research and Development, Groton, Connecticut, United States.

Methods

Single crystal X-ray diffraction

Single crystal X-ray measurements were conducted on a Rigaku Rapid II curved image plate diffractometer with a Cu-K α X-ray microsource ($\lambda = 1.54178 \text{ \AA}$) with a laterally graded multilayer (Goebel) mirror for monochromatization. Single crystals were mounted on Mitegen microloop mounts using a trace of mineral oil and cooled in-situ to 100(2) K for data collection. Data were collected using the dtrek option of CrystalClear-SM Expert 2.1 b32 [1]. Data were processed using HKL3000 [2] and data were corrected for absorption and scaled using Scalepack [2]. The space group was assigned and the structures were solved by direct methods using XPREP within the SHELXTL suite of programs [3] and refined by full matrix least squares against F^2 with all reflections using Shelxl2014 [4] with the graphical interface Shelxle [5]. The

crystal under investigation was found to be non-merohedrally twinned. HKL3000 lacks the ability to simultaneously integrate more than one twin domain. Rigaku programs compatible with the diffractometer (twinsolve) gave unsatisfactory results. The data were thus instead handled as if not twinned, with only the major domain integrated, and converted into an hklf 5 type format hkl file after integration using the "Make HKLF5 File" routine as implemented in the program WinGX [6]. The twin law and matrix were obtained using the program ROTAX as implemented in WinGX. The twin operation was identified as a 180° rotation around the reciprocal a-axis, the twin matrix as 1 0 1.313, 0 -1 0, 0 0 -1. The Overlap R1 and R2 values in the "Make HKLF5 File" routine used were 0.23, i.e. reflections with a discriminator function less or equal to overlap radius of 0.23 were counted overlapped, all others as single. The discriminator function used was the "delta function on index non-integrality". No reflections were omitted.

The structure was solved using direct methods with all reflections of component 1. The structure was refined using the hklf 5 routine with all reflections of component 1 (including the overlapping ones) as obtained from WinGX, resulting in a BASF value of 0.297(3). No R_{int} value is obtainable for the hklf 5 type file using the WinGX routine.

H atoms attached to carbon and nitrogen atoms were positioned geometrically and constrained to ride on their parent atoms, with carbon hydrogen bond distances of 0.95 Å for aromatic and alkene H atoms, 0.99 Å for CH₂, 0.88 Å for NH, and 0.98 Å for CH₃ moieties, respectively. Methyl H atoms were allowed to rotate but not to tip to best fit the experimental electron density. Water H atoms were freely refined with O-H bond distances restrained to 0.84(2) Å. $U_{\text{iso}}(\text{H})$ values were set to a multiple of $U_{\text{eq}}(\text{C/N/O})$ with 1.5 for OH and CH₃, and 1.2 for N-H, C-H and CH₂ units, respectively.

Table 1. Experimental details

	MICONZ04 (MM dihydrate)
Crystal data	
Chemical formula	$C_{18}H_{15}Cl_4N_2O \cdot CH_3O_3S \cdot 2(H_2O)$
Moiety formula	$C_{18}H_{15}Cl_4N_2O$, CH_3O_3S , 2 H_2O
M_r	548.24
Crystal system, space group	Monoclinic, $C2/c$
Temperature (K)	100
a, b, c (Å)	38.449 (3), 9.0878 (5), 13.6903 (9)
β (°)	103.528 (5)
V (Å ³)	4650.9 (5)
Z	8
$F(000)$	2256
D_x (Mg m ⁻³)	1.566
Radiation type	Cu $K\alpha$
No. of reflections for cell measurement	39176
θ range (°) for cell measurement	4.7–73.5
μ (mm ⁻¹)	5.82
Crystal shape	Plate
Colour	Colourless
Crystal size (mm)	0.12 × 0.06 × 0.02
Data collection	
Diffractometer	Rigaku Rapid II curved image plate diffractometer
Radiation source	microfocus X-ray tube
Monochromator	Laterally graded multilayer (Goebel) mirror
Scan method	ω scans
Absorption correction	Multi-scan, <i>SCALEPACK</i> (Otwinowski & Minor, 1997)
T_{\min}, T_{\max}	0.465, 0.893
No. of measured, independent and observed [$I > 2\sigma(I)$] reflections	39176, 39176, 33902
R_{int}	n/a
θ values (°)	$\theta_{\max} = 72.4$, $\theta_{\min} = 4.7$
$(\sin \theta/\lambda)_{\max}$ (Å ⁻¹)	0.618

Range of h, k, l	$h = -47 \rightarrow 47, k = -11 \rightarrow 11, l = -16 \rightarrow 16$
Refinement	
Refinement on	F^2
$R[F^2 > 2\sigma(F^2)], wR(F^2), S$	0.070, 0.205, 1.05
No. of reflections	39176
No. of parameters	303
No. of restraints	4
H-atom treatment	H atoms treated by a mixture of independent and constrained refinement
Weighting scheme	$w = 1/[\sigma^2(F_o^2) + (0.0633P)^2 + 49.6689P]$ where $P = (F_o^2 + 2F_c^2)/3$
$(\Delta/\sigma)_{\max}$	0.001
$\Delta\rho_{\max}, \Delta\rho_{\min}$ (e \AA^{-3})	0.85, -0.82

Figures

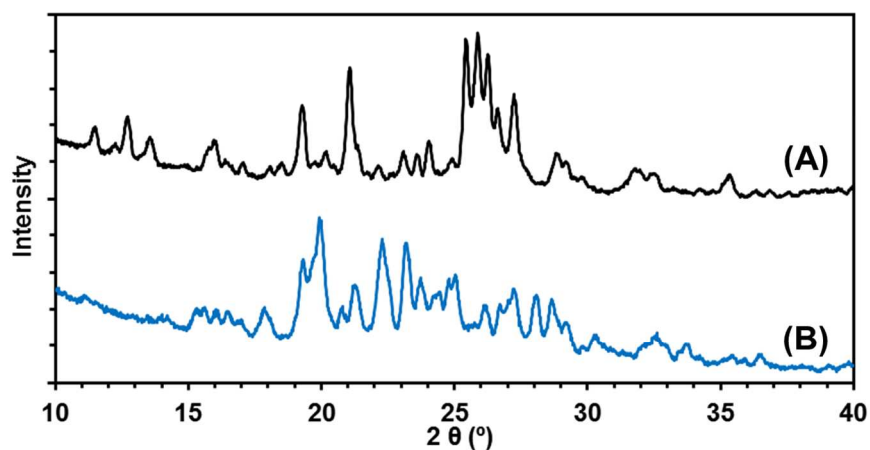


Figure S1. XRPD pattern of (A) MCZ and (B) AH.

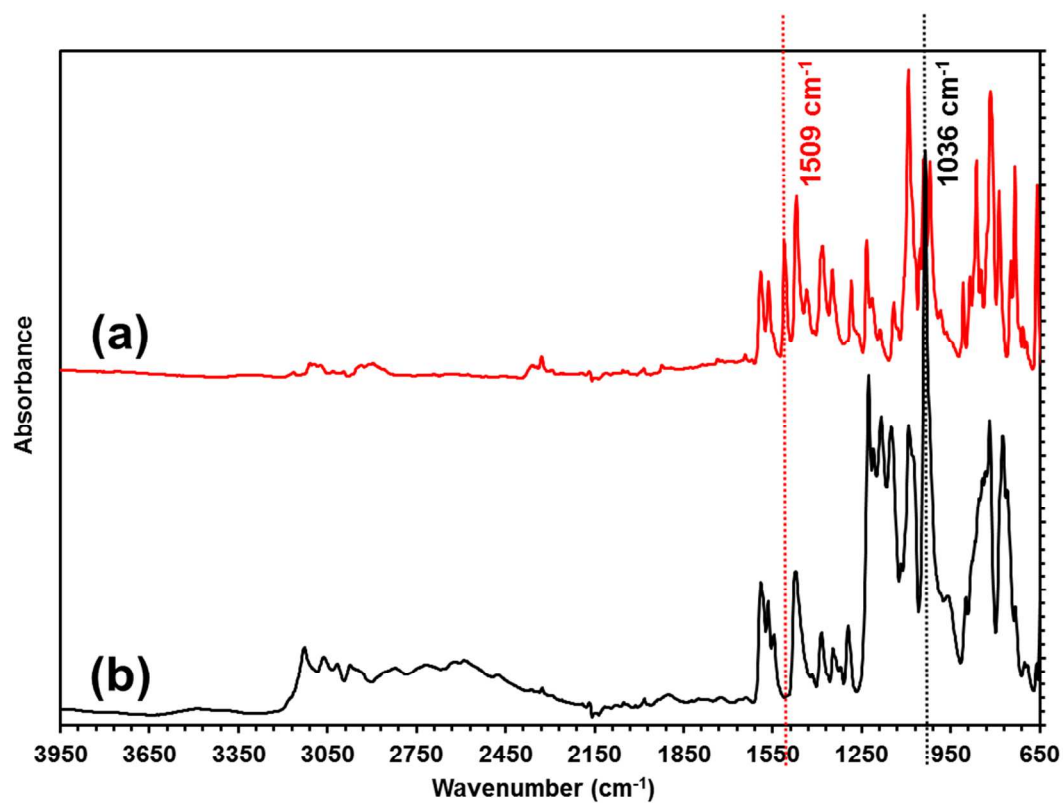


Figure S2. FTIR spectrum of (a) MCZ and (b) AH. The dotted vertical lines at 1509 cm^{-1} and 1036 cm^{-1} represents unique peaks of MCZ and AH, respectively.

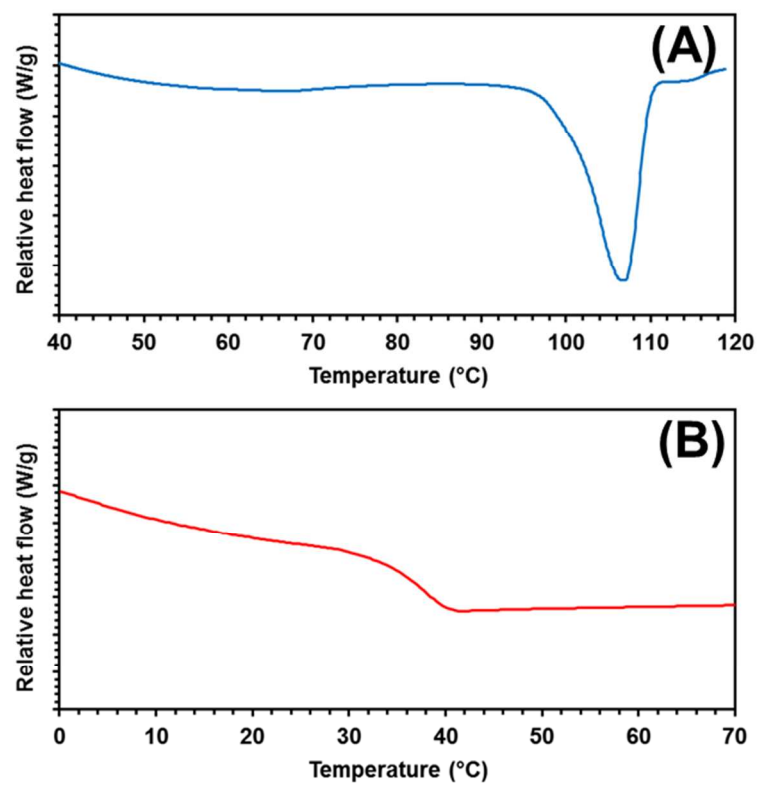


Figure S3. DSC traces of (A) AH and (B) AMO.

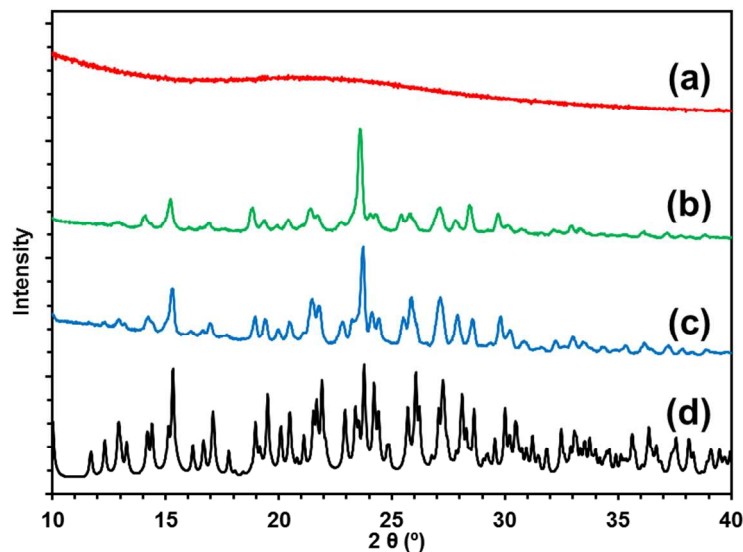


Figure S4. XRPD pattern of (a) AMO stored in a desiccated container for 4 weeks at 25 °C, (b) AMO stored in 57 % RH for 2 days at 25 °C (c) AH stored in 75 % RH for 2 days at 25 °C, and (d) calculated XRPD pattern from DH single crystal structure.

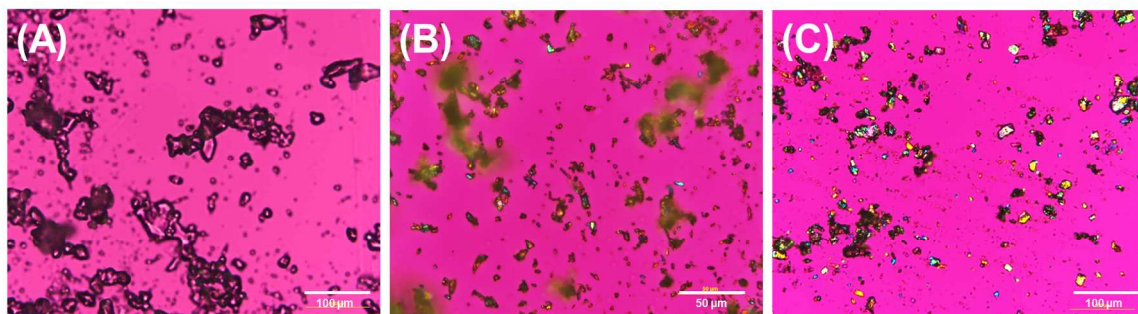


Figure S5. Polarized light microscopic images of (A) AMO, (B) AH, and (C) DH.

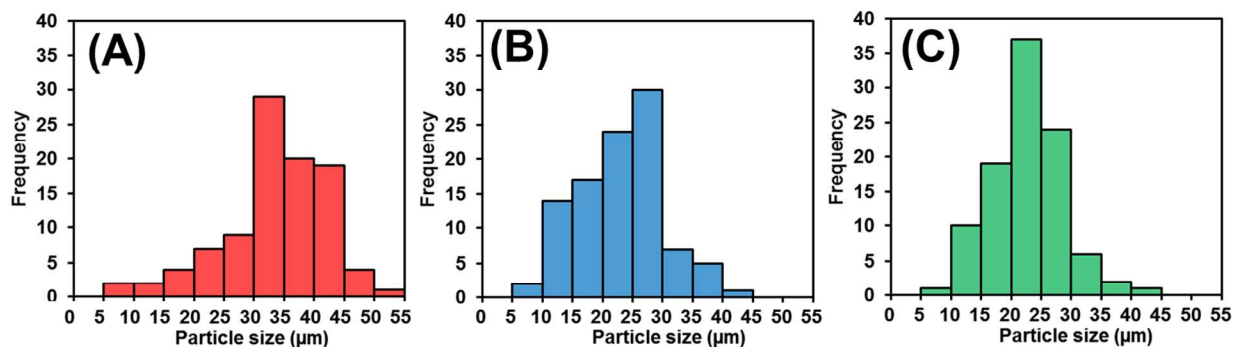


Figure S6. Particle size distribution for (A) AMO, (B) AH, and (C) DH.

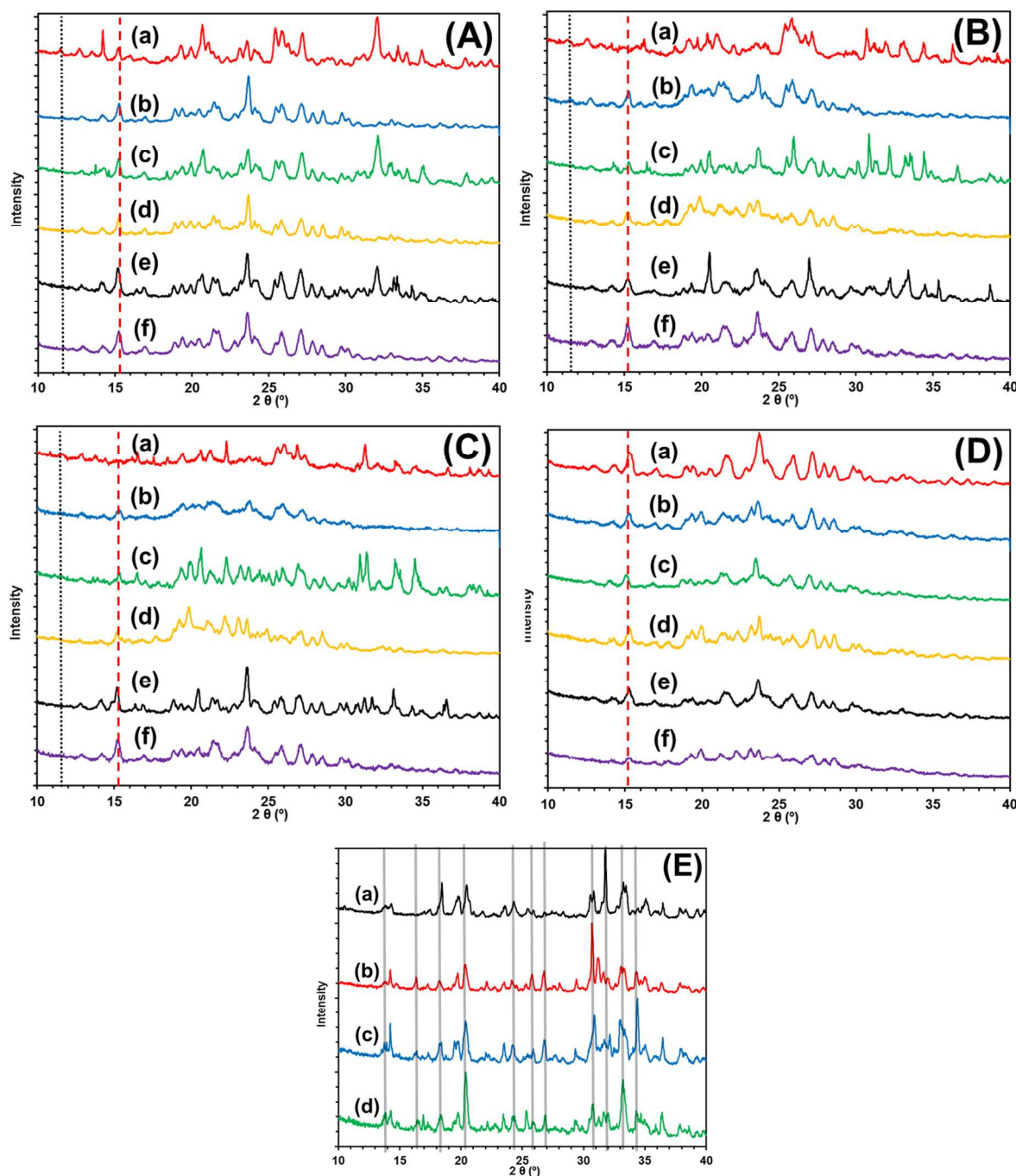


Figure S7. XRPD patterns for various sample after storage for 2 days at (A) at 57 % RH, (B) at 43 % RH, and (C) at 33 % RH for (a) AMO + TSPd, (b) AMO + CCS, (c) AH + TSPd, (d) AH + CCS, (e) DH + TSPd, and (f) DH + CCS; (D) control samples of (a) neat AMO at 57 % RH, (b) neat AH at 57 % RH, (c) neat AMO at 43 % RH, (d) neat AH at 43 % RH, (e), neat AMO at 33 % RH, and (f) neat AH at 33 % RH. (E) Samples for TSPd stability analysis (a) neat TSPd at 33 % RH, (b) neat TSPd at 43 % RH, (c) neat TSPd at 57 % RH, and (d) neat TSPd before storage. The dotted and dashed lines indicate the position of unique peak for MCZ and DH, respectively.

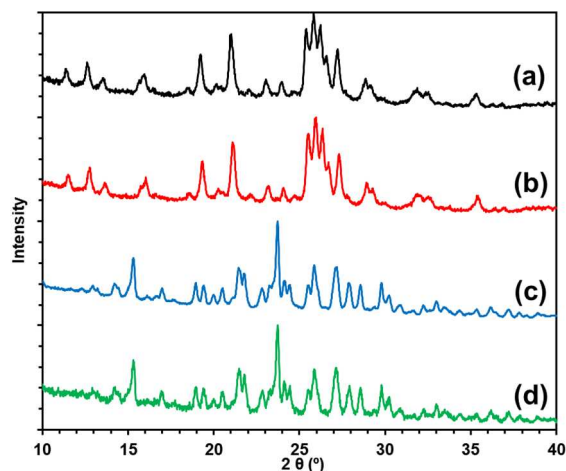


Figure S8. XRPD pattern of (a) neat DH, (b) neat DH after exposure to 57 % RH for 7 days, (c) neat MCZ, and (d) neat MCZ after exposure to 57 % RH for 7 days.

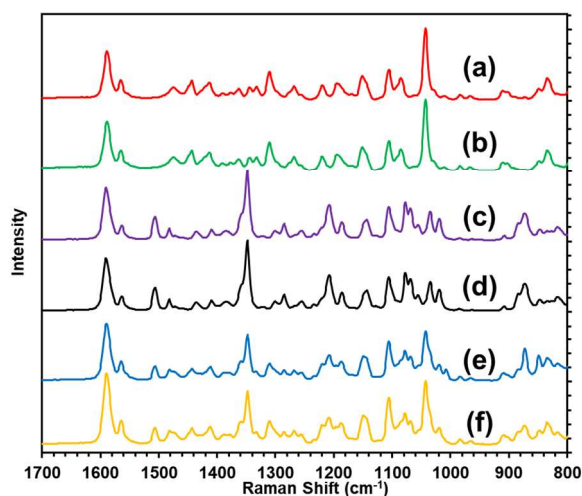


Figure S9. Raman spectra of (a) neat DH, (b) neat DH after exposure to 57 % RH for 7 days, (c) neat MCZ, (d) neat MCZ after exposure to 57 % RH for 7 days, (e) DH + MCZ (1:1) mixture, and (f) DH + MCZ (1:1) mixture after exposure to 57 % RH for 7 days. The composition of the mixture of the DH (50 mole %) and MCZ (50 mole %) did not change upon storage at 57 % RH for 7 days.

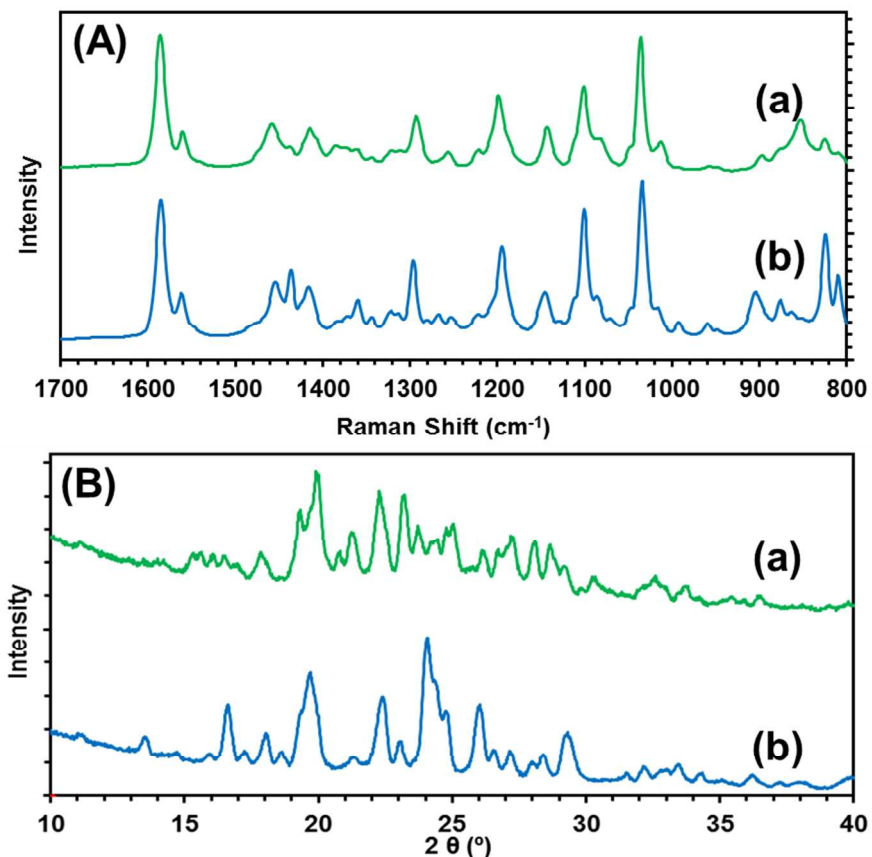


Figure S10. (A) Raman and (B) XRPD spectra of (a) MM solid form used in this study and (b) MM solid formed obtained by following method described in Guerrieri *et. al* (2009).

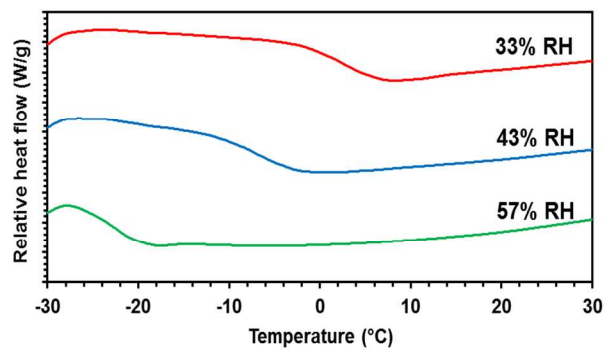


Figure S11. DSC traces of AMO stored at 33 % RH, 43 % RH, and 57 % RH.

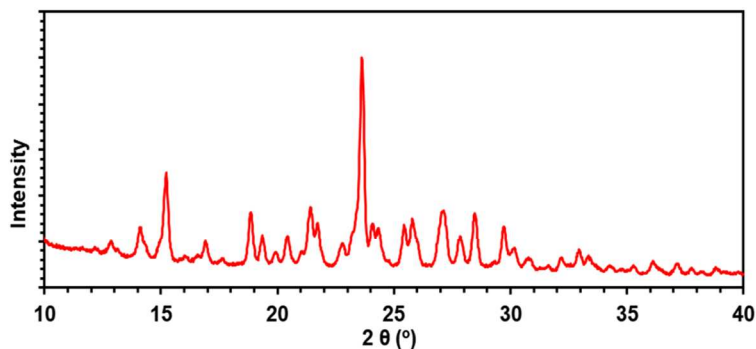


Figure S12. XRPD pattern of solid residues obtained after slurring DH in water for 2 days.

References

- [1] Rigaku Corp., The Woodlands, Texas, USA.
- [2] Otwinowski Z, Minor W., Processing of X-ray diffraction data collected in oscillation mode. *Methods Enzymol.* **1997**, 276, 307–326.
- [3] a) SHELXTL suite of programs, Version 6.14, 2000-2003, Bruker Advanced X-ray Solutions, Bruker AXS Inc., Madison, Wisconsin: USA) b) Sheldrick GM. A short history of SHELX. *Acta Crystallogr A.* **2008**, 64(1), 112–122.
- [4] a) Sheldrick GM. University of Göttingen, Germany, **2013**. b) Sheldrick GM. Crystal structure refinement with SHELXL. *Acta Crystallogr Sect C Struct Chem.* **2015**, 71(1), 3–8.
- [5] Hübschle CB, Sheldrick GM, Dittrich B. ShelXle: a Qt graphical user interface for SHELXL. *J. Appl. Crystallogr.* **2011**, 44(6), 1281–1284.
- [6] Farrugia, LJ, *J. Appl. Crystallogr.* **2012**, 45, 849-854.